SIMULATIONS OF OROGRAPHIC FLOWS WITH A 10 KM - SCALE HYDROSTATIC MODEL

P. Bougeault
EERM/CNRM, Toulouse, France

1. INTRODUCTION

As horizontal resolution increases, the primitive-equation models which are presently used for operational NWP become able to resolve a larger part of the earth orography, and of the associated meso-scale circulations. It is therefore necessary to assess to which extent they are able to deal with these new processes. The success in the simulation of meso-β-scale patterns is not granted by the fact that a model performs well on Rossby waves, since these new flows involve rapidly propagating waves with smaller vertical wavelengths and local dissipative processes. As part of the qualification of the French Weather Service LAM Péridot for the meso-β-scale (Δx=10 km), two-dimensional simulations of orographic flows are currently assessed which reveal the good performance of the model, given some modifications (Bougeault, 1987a, 1987b). These results have important implications for the present workshop, since they anticipate on the work which will become necessary if the ECMWF model resolution increases. Thus, in contrast with other contributions in this workshop, this paper will not deal with new techniques, but with the ability of present day techniques to deal with orographic flows, which should be preserved when changing to new ones. A short review of on-going work on the radiating upper boundary conditions will be given in Section 2, without connection with the remainder of the paper. Section 3 will briefly present the model, the necessary modifications and a linear test. In Section 4 we assess the model results in three real cases. Some sensitivity studies are shown in Section 5. Implications of the results are analysed in Section 6.

2. A SHORT REVIEW OF THE UPPER BOUNDARY CONDITION PROBLEM

It is well established that at the top of any numerical model, wave energy should only propagate upward, without reflection. Klemp and Lilly (1978) have shown that it is not possible to achieve this property in the context of a "local" (in space and time) formulation, since for internal atmospheric waves phase and energy propagate in opposite directions in the vertical. They have proposed to use a "damping layer" to achieve the same effect. In the damping

layer approach, several model levels are used to dissipate wave energy propagating upward, by use of a slowly growing diffusion or Rayleigh damping. This method is easy to implement and has been used widely since then, at the expense of increased computational cost.

In the recent past however, some methods have been proposed to overcome the problem due to the "non-local" character of the radiating UBC. Bougeault (1983) and Klemp and Durran (1983) have noticed that, for pure gravity waves in a simple mean environment, it is possible to give a formulation involving only the horizontal Fourier transforms of the pressure and vertical velocity fields. Let

$$\tilde{p}(\underline{k},z,t) = \int p(x,z,t)\, e^{i\underline{k}\cdot\underline{x}}\, dx \ ,$$

$$\tilde{w}(\underline{k},z,t) = \int w(x,z,t)\, e^{i\underline{k}\cdot\underline{x}}\, dx \ ,$$

be these quantities. Then, the radiative UBC reads

$$\tilde{p}(\underline{k},z,t) = \frac{N}{|\underline{k}|}\, \tilde{w}(\underline{k},z,t) \ , \qquad (1)$$

where N is the Brunt-Väisälä frequency. Thus, for a model using z coordinates, it is easy to diagnose W at the top, at each time step, to compute p by (1), and to enter the result in the U-momentum equation at the same level.

Alternative formulations of (1) read

$$\nabla_{\underline{h}} \tilde{p} = \frac{i\underline{k}}{|\underline{k}|}\, N\, \tilde{w} \ , \qquad (2)$$

whereby the pressure gradient at the top of the model can be directly computed, or

$$\tilde{\omega} = -\frac{\underline{k}}{Ng}\, \tilde{\Phi} \qquad (3)$$

for the models using the pressure coordinate system (Φ being the geopotential, and $\omega = \frac{dp}{dt}$). Furthermore, Bougeault (1983) showed that it is possible to use (1) within the framework of the semi-implicit treatment of the gravity waves, widely used in the present primitive equation models. Since then, several

studies have demonstrated the effectiveness of this approach for meso-scale models (e.g. Brière, 1987; Schumann, 1987; Durran, 1987 and others).

A generalization of (2) to the case of inertia-gravity waves on a f-plane has been proposed by Garner (1986) with a remarkably simple formulation. Let f be the Coriolis parameter, $\underline{u}_{rot}$ the rotational part of the horizontal wind and $\underline{z}$ the vertical unit vector, then (2) is generalized by

$$\nabla_{\underline{h}} \tilde{p} = \frac{i\underline{k}}{|\underline{k}|} N \tilde{w} - \frac{1}{2} f \, \underline{z} \times \underline{u}_{rot} \qquad (4)$$

which can be implemented at virtually no increase of cost.

Based on the Parseval theorem for the Fourier transform, Garner (1986) also proposed a formulation of (2) which does not involve Fourier transforms at each time step. Let $p_x(x)$ be the finite difference form of the horizontal pressure gradient at the model top boundary. Then the discrete analog of (2) is given by

$$p_x(x) = \frac{N}{\pi} \sum_{n'} w(x_{n'}) \, H(x_{n'}-x) \, \Delta x, \qquad (5)$$

where the summation extends over all grid points of the top model level, and H(x) is a weight function depending on the distance between the two grid-points only. Thus, the weights $H(x_n)$ can be computed and stored once and for all at the beginning of the model integration.

Finally, Rasch (1986) has given a fairly complete discussion of the UBC problem, and shown that the above-mentioned solutions are part of a family which can be obtained for any system of equations, using a broad strategy based on the work by Enquist and Majda (1977, 1979). The method can be summarized as follows, and applies to any system of equations:

(1) write the dispersion equation of the system;

(2) solve for σ, the intrinsic frequency, and retain only the solution propagating energy upward. This solution will be, in the general case, non local with respect to z and t (contrary to (1)).

(3) Find a judicious approximation to the solution through a rational function, using asymptotic developments based on the order of magnitude of σ.

(4) Use symbolic calculus techniques to associate with the approximate form of σ a set of partial differential equations local in z and t having the same dispersion equation. This may involve the definition of new "ad-hoc" quantities, describing in broad terms, the "activity" of the waves.

Rasch (1986) applies this method to the case of Rossby and gravity waves on a β-plane and claims that it is possible to approximate the radiative UBC by introducing no more than 4 new prognostic variables at the top of the model. The amount of computations involved is therefore much smaller than in a damping layer. This approach seems therefore to be very promising for limited-area β-plane models, for which it would allow to save many upper levels.

There remain several problems in the definition of the radiative UBC. Formulations (1) to (5) are, strictly speaking, valid for periodic problems. Until now, only ad-hoc methods have been used to apply them to non-periodic cases. Also, no formulation exists when the Brunt-Väisälä frequency is varying significantly across the domain where the Fourier transform is taken.

Moreover, no solution has yet been proposed for the full atmospheric problem over the sphere. Recent results by Cariolle (1987) clearly show that some of the deficiencies in the climatology of global models might be related to the reflection of Rossby waves at the top boundary. The use of a damping layer which extends over several layers is, at the present time, the only way to prevent this reflection.

Note that this last approach is effective only if the model vertical grid resolves the waves well into the absorption area. If this condition is not met, the waves are reflected downward by the course grid before being damped. This pleads in favour of largely increased resolution in the stratosphere as compared to the present status in operational NWP models. There are clear benefits in treating explicitly the dynamics of the stratosphere in global

models, and this may well reject the problem of the radiative UBC on the sphere to a low order of priority.

None of the techniques discussed in this Section applies to models using terrain-following coordinates (they would, however, apply to a hybrid coordinate system). Therefore for the remainder of the paper, we will use the damping layer approach.

3. MODEL FORMULATION AND TEST OF THE LINEAR SOLUTION

The model used is a two-dimensional version of the French Weather Service LAM Péridot. A complete description of the model is given by Imbard et al., (1986) and Bougeault (1986). The model uses the primitive equation system, and a σ-vertical coordinate. The discretization on the horizontal follows the Arakawa C-grid. On the vertical, all the dependent variables (T, U) are at the same level, and the vertical velocity ($\dot{\sigma}$) is computed at mid-levels. The time discretization uses the classical semi-implicit treatment of the gravity waves.

The model is made two-dimensional by using an elongated horizontal grid (43x3 points), and enforcing the condition $\frac{\partial}{\partial y} = 0$ at y lateral boundaries. At the x boundaries, the operational relaxation scheme towards specified values is maintained. The horizontal resolution for the experiments shown here is $\Delta x = 5$ km. 40 levels are used on the vertical, with a regular z distribution ($\Delta z = 500$ m). The time step is $\Delta t = 30$ s. The damping zone is defined in the higher 10 levels.

The most important modification made to the operational code concerns the formulation of the horizontal diffusion operator. In the operational model, as in most models at the present time, the diffusion operator applies along σ-surfaces. To correct for this inaccuracy, the diffusion acts on θ instead of T. Thus, the formulation for T reads:

$$\frac{\partial T}{\partial t} = k_2 \, p_s^k \, \nabla_\sigma^2 \, (p_s^{-k} \, T). \qquad (6)$$

In the stratosphere, where the temperature is nearly isothermal, this formulation is worse than a simple diffusion of T along σ-surfaces. Therefore, in the present runs, we use the better formulation:

$$\frac{\partial T}{\partial t} = k_2 \, \nabla_p^2 \, T \qquad (7)$$

This involves a lot of vertical interpolations at each time step, but considerably improves the model results, as will be shown below (see Section 5.2).

The model physics is described by Bougeault (1986). For the experiments shown here, only the vertical diffusion scheme is retained. This involves friction at the bottom, with a surface roughness parameter Z_o and diffusion from level to level. The formulation generally follows Louis et al., (1981).

The model dynamics is tested by comparing the results to a linear analytical solution, in the way used before by many authors. A bell-shaped mountain is used $h(x) = h_o/(1+x^2/a^2)$, with a half-width a=25 km, and h_o small. The results are then amplified to get the linear solution for h_o = 500 m. The atmospheric basic state is assumed isothermal (T=273.15 K) with uniform mean wind (U=20 m/s). The analytical solution (Alaka, 1960) is shown in Fig. 1a (horizontal velocity only). The model is integrated to steady-state and the results are shown in Figs. 1b-d. In Fig. 1b the operational vertical grid using 15 irregularly spaced levels has been used, and there is no damping layer. The model performance is quite poor, and one clearly distinguishes a pattern of reflection. In Fig. 1c, the high resolution vertical grid has been used, together with the damping layer, and the result is now acceptable. In Fig. 1d, the high-resolution grid has been used without the damping layer, and the result is still worse than in case 1b. Thus, it is absolutely necessary both to increase the resolution and to include a damping layer to achieve a good result. Furthermore, the higher the resolution, the more the results suffer from the absence of damping. In the following, the model configuration used in 1c is retained.

4. THREE CASE STUDIES

4.1 The flow over the Rocky Mountains on 17-02-1970

This case has been documented observationally by Lilly and Kennedy (1973), and simulated by Klemp and Lilly (1978) and Hoinka (1985). We have used the upstream sounding given by Klemp and Lilly to define the initial state in the model. The tropopause is very high, and the wind is very strong (60 m/s) in the upper troposphere. A comparison of observed and simulated wind vertical cross-section is given at Fig. 2. The simulation is quite satisfactory, as exemplified by the behaviour of isolines 30 m/s and 50 m/s. The formation of

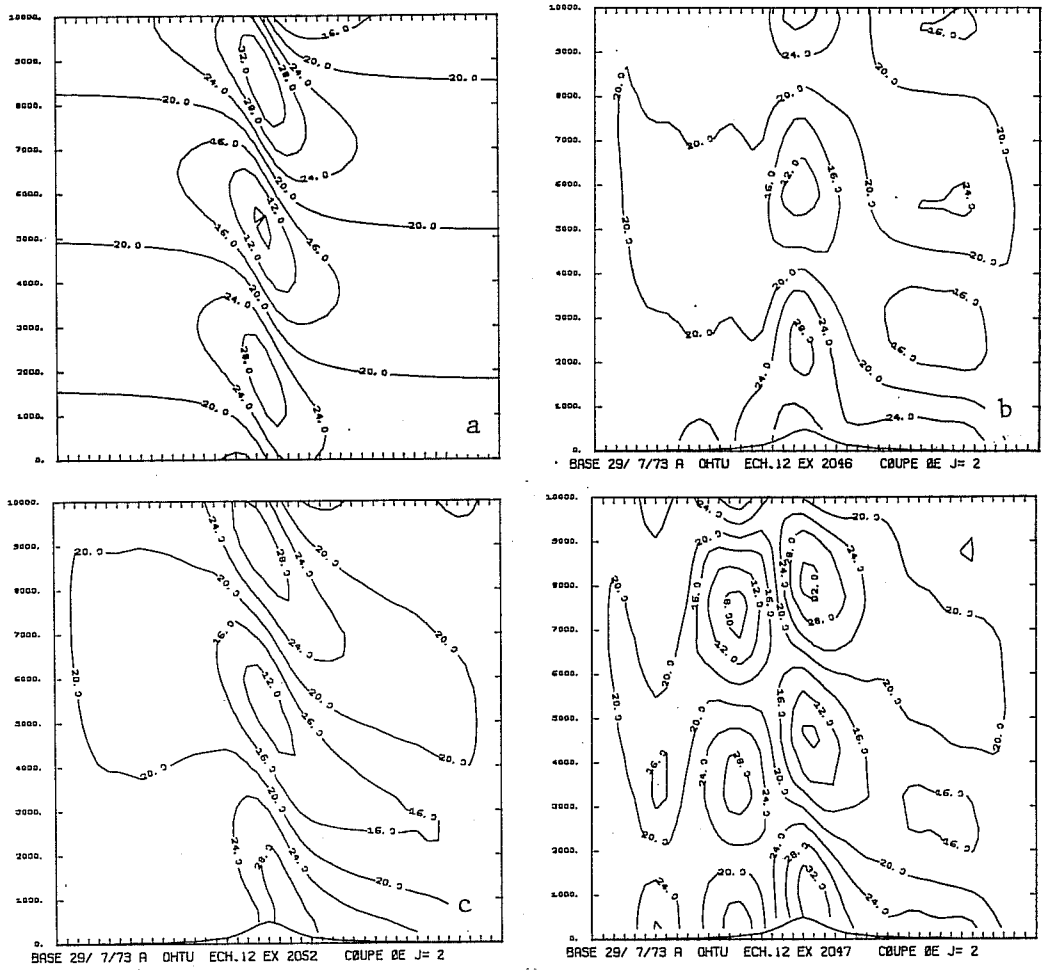

Fig. 1 Comparison between the linear, analytical solution (a), and the model results for various configurations (b-d).

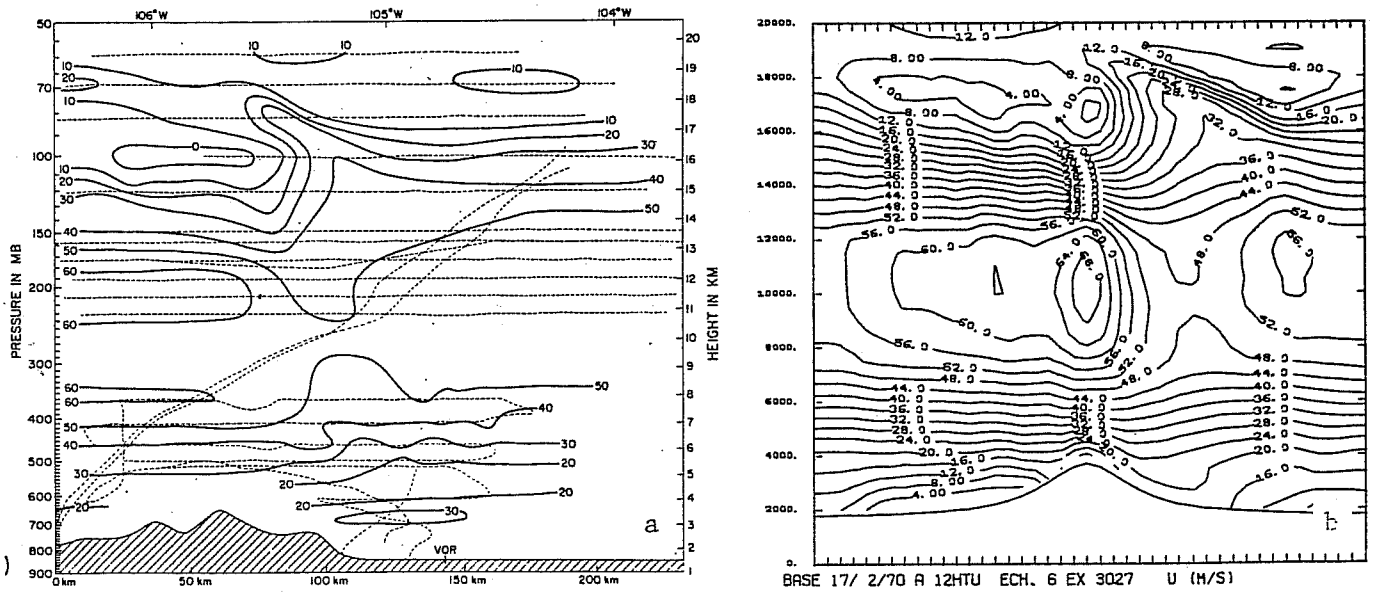

Fig. 2 Vertical cross-section of the wind for 17/2/70 (a) observed, (b) simulated.

a blocking zone upstream of the crest, just below the tropopause, is well captured by the model, although quantitatively underestimated.

A parameter generally used to assess the quality of the mountain wave simulation is the vertical momentum flux

$$M = \frac{1}{L} \int_L \rho \, \overline{u'w'} \, dx \ , \qquad (8)$$

where the summation extends over an arbitrary length L across the mountain range. This quantity has been computed for the model and the observations, using L=200 km, and the comparison is shown at Fig. 3. The model result is around -0.5 Pa, whereas observations oscillate around -0.6 Pa. This can be considered as a reasonably good agreement. Both model and observations indicate a constant value throughout the troposphere and an abrupt decrease towards zero near 16 km altitude. This is generally interpreted as the sign of wave absorption by the (non-linearly induced) critical level below the tropopause. Strong turbulence has been observed near 16 km, confirming this hypothesis.

4.2 The flow over the Dynaric Alps on 6-03-1982

A fairly detailed analysis of the Bora event observed on 6-03-1982 during ALPEX has recently been given by Pettré (1987). The upstream sounding exhibits a well marked inversion at 3 km, which coincides with a rotation of the wind from NE to SE, thereby creating a linear critical level at 4 km for waves perpendicular to the SE-NW oriented ridge. To simulate this low-level case, the model vertical increment is reduced to ΔZ=250 m. A comparison of model results and observations is given in Fig. 4. The linear critical level is well visible both in the observations (Fig. 4a) and the model (Fig. 4b). Below this level, the model results are in general agreement with the observations. The model produces a "shooting flow" of limited extension on the steep down-wind slope. However, it underestimates the return flow, well visible at 4 km on the observations. Above the critical level, the agreement is not so good. Strong upward velocities are observed near 5 km just above the ridge, without counterparts in the model results. The reason for this discrepancy is not yet understood. Note that Klemp and Durran (1987) have presented some Bora simulations with a non-hydrostatic model that are qualitatively very similar to the one shown here.

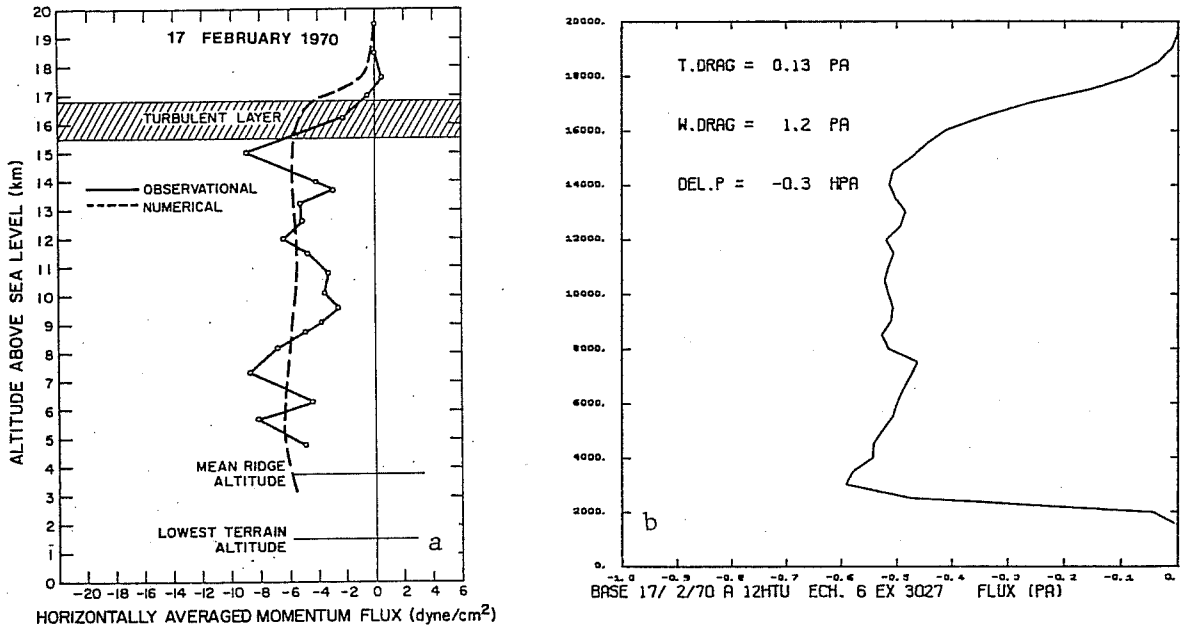

Fig. 3 Observed (a) and simulated (b) vertical flux of momentum for 17/2/70.

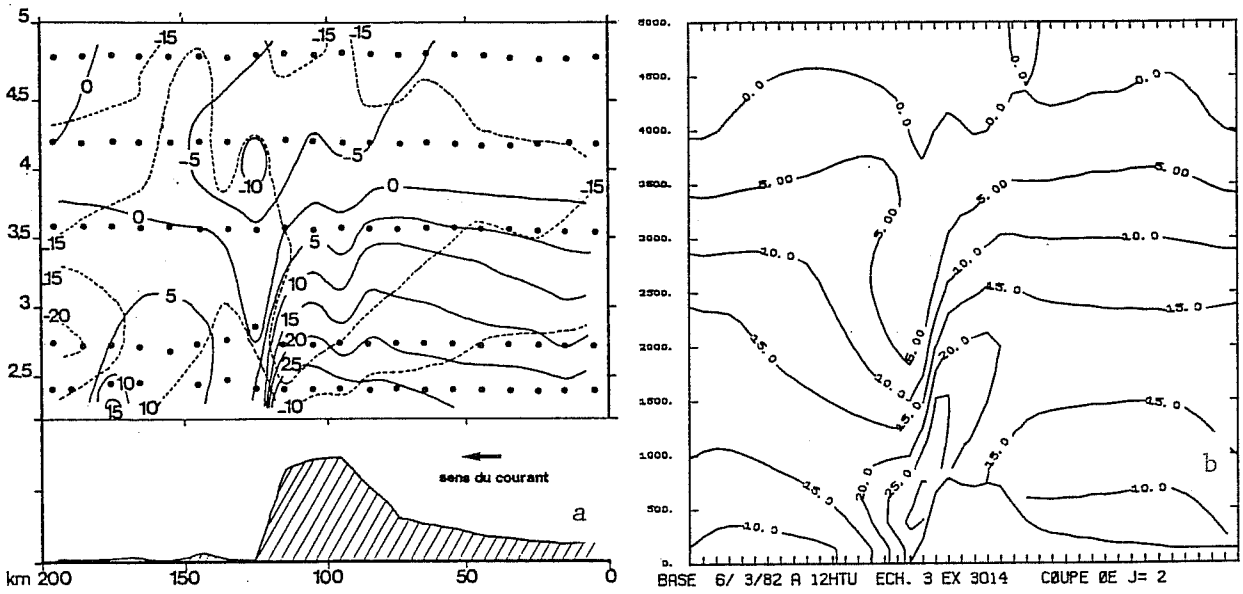

Fig. 4 Vertical cross-section of the wind for 6/3/82: (a) observed, (b) simulated.

4.3 The Chinook event of 11-01-1972

Many authors have simulated the extreme Chinook event observed near Boulder, Colorado, on 11-01-1972, and described by Lilly (1978). Klemp and Lilly (1978), and Hoinka (1985) have obtained reasonably good simulations with hydrostatic models, whereas Peltier and Clark, (1979) and Durran and Klemp (1983) have used non-hydrostatic models. There are three competing theories to explain the formation of this windstorm. As summarized by Durran (1987), these theories are:

(i) The constructive interference of wave components reflected against the low level inversion and the tropopause, according to the linear theory (Klemp and Lilly, 1975).

(ii) The trapping of wave energy between the ground and a non-linear critical level induced by the wavy breaking in the lower stratosphere (Peltier and Clark, 1979).

(iii) The internal hydraulic theory, which states that shooting flows should occur when the "internal Froude number" reaches a critical value of 1 at the top of the mountain. Results supporting this explanation have been obtained by Smith (1985) and Durran (1986, 1987).

To simulate this event, the upstream sounding is taken from the material published by Klemp and Durran (1983). The temperature sounding exhibits a "low level" inversion between 500 hPa and 600 hPa. The mountain range is schematized by a bell-shaped mountain with half-width a = 10 km.

The model physics uses z_o=0.04 m and K2=6Δx. A comparison between the model predicted and observed wind fields is shown at Fig. 5. The model succeeds remarkably at forecasting the intense downslope windstorm, and the breaking wave in the high troposphere, negative values of the wind being simulated between 10 and 13 km. The vertical velocities associated with these extreme values reach ± 10 m/s in the simulation. The hydrostatic approximation is clearly questionable in this case. However, examination of the model-forecasted parameters shows a great similarity with these results obtained by the afore mentioned non-hydrostatic models.

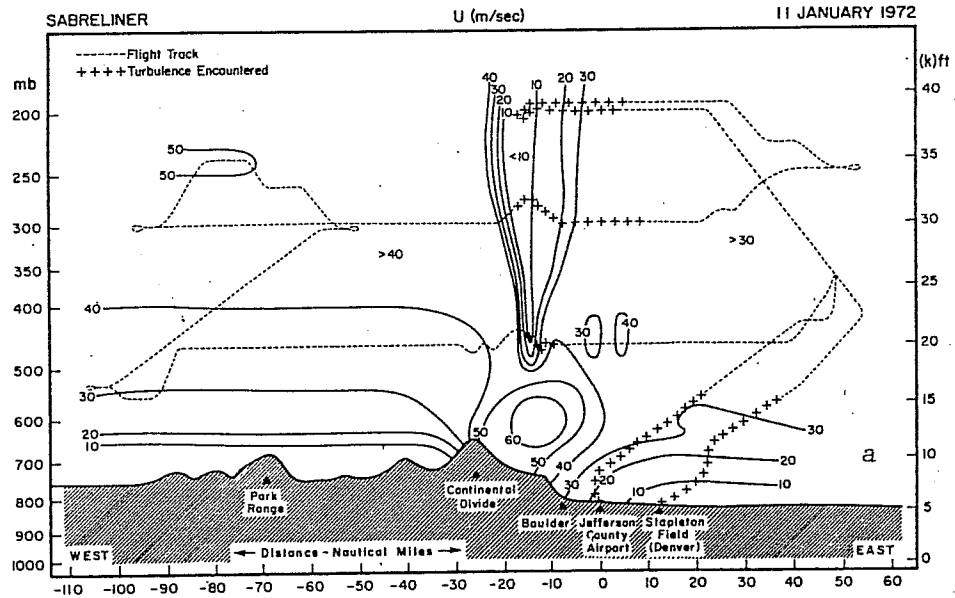

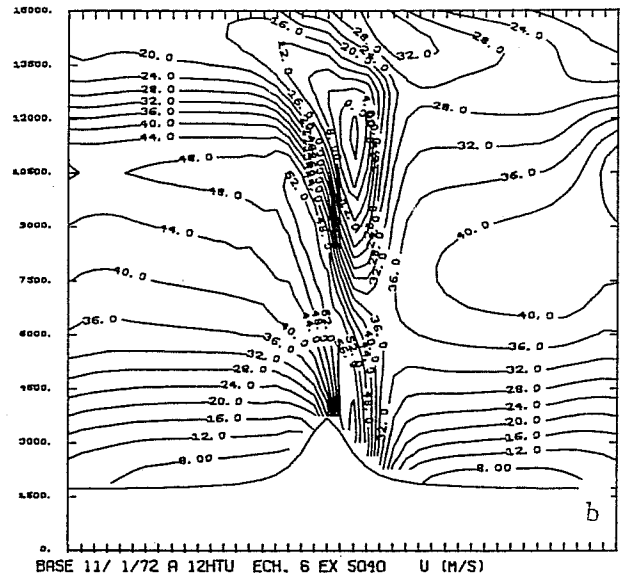

Fig. 5 Vertical cross-section of the wind for 11/01/72: (a) observed, (b) simulated.

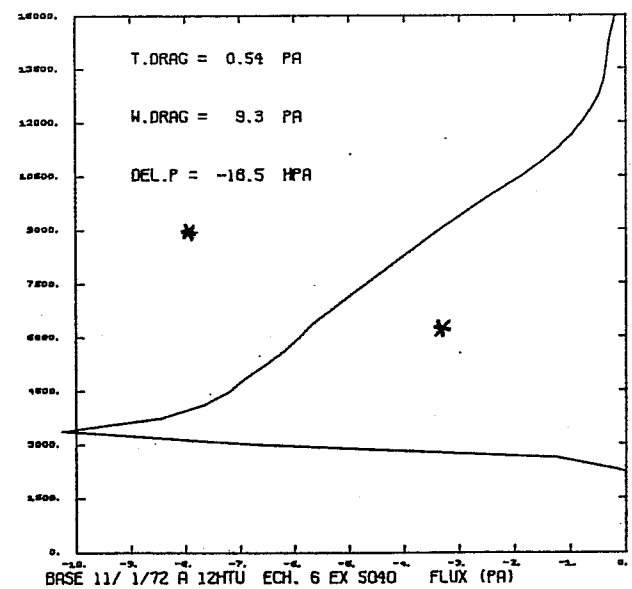

Fig. 6 Observed (X) and simulated (—) vertical flux of momentum for 11/01/72

For instance, the pressure drag at the surface has been computed according to:

$$D = \frac{1}{L} \int_0^1 p_s \frac{\partial h}{\partial x} dx \ , \qquad (9)$$

with L = 200 km. The model gives a value of 9.2 Pa for this quantity. Both Klemp and Durran (1983) and Peltier and Clark (1979) have obtained around 8 Pa. Furthermore, this value is in good quantative agreement with the momentum flux M computed according to Eq. (8) (see below). The pressure difference between two points located at altitude 2600 m upstream and downstream of the crest reaches -18.5 hPa in our simulation, whereas Lilly (1978) mentions the observed value of -12 hPa.

The vertical flux of horizontal momentum (M) is shown in Fig. 6, together with observational estimates of Lilly. The value of the flux decreases linearly throughout the troposphere, and is commensurate with direct aircraft measurement, given the uncertainty of these measurements.

In summary, all three simulations are quite realistic, and come close to results obtained with research models.

5. SENSITIVITY STUDIES

The model results exhibit a marked sensitivity to several parameters. A fundamental problem for this workshop is of course the minimal vertical resolution necessary to achieve the above mentioned results, and the adequacy of the damping layer procedure. Concerning the vertical resolution, several tests (not shown here) have led to the conclusion that an acceptable minimal resolution would be a constant Δz=1 km throughout the troposphere and lower stratosphere. In particular, it is necessary to resolve correctly the tropopause region, where many important phenomena can occur, such as partial reflection or absorption by a non-linear critical level. In view of these results, one may also recommend to use constant Δz increments rather than variable ones, since as Δz changes with height, some wave components which are resolved in the lower stratosphere become unresolved, and may experience reflection.

Concerning the damping layer effectiveness, in contrast with the result shown in Fig. 1d, the model results were found quite insensitive to the presence or absence of this damping level in all three cases analysed in Section 4. One may argue that the waves are absorbed by a non-linear critical level in case 4.1, by a linear critical level in case 4.2, and that they are reflected at the tropopause level in case 4.3. So, in all three cases, there is a physical reason for wave energy not propagating beyond a given level, which might not be the general case.

Beside this, we will report some results on the sensitivity to (i) the mean profiles, (ii) the formulation of the horizontal diffusion, (iii) the roughness length.

5.1 Sensitivity to the mean profiles

The model shows a marked sensitivity to the definition of the mean profiles of U and T. For most cases, this sensitivity is restricted to the quadratic parameters, such as the vertical momentum flux M. An example of this "weak" dependence is shown in Fig. 7, on case 4.1. Fig. 7a is the control run shown above. In Fig. 7b, the upstream wind has been increased by 10% in the layer between 200 and 300 hPa. The equilibrium value of the flux is reduced by a factor 2. This highlights the difficulty of comparing direct observational estimates of this quantity and model results, given the uncertainty on upstream profiles.

In some cases however, the sensitivity is still more important: the occurrence or non-occurrence of the downslope windstorm itself can be governed by small changes in the upstream profiles. An example of this extreme dependence is shown in Fig. 8 (case 4.3). The cross-sections of θ are shown for several modifications of the reference profiles. In Fig. 8a, the stratospheric wind has been increased from 20 m/s to 40 m/s. As suggested by Peltier and Clark (1979), and already confirmed by Hoinka (1985), this results in preventing the wave breaking in the lower stratosphere, and the wind-storm is suppressed. In Fig. 8b, the low-level inversion has been removed from the upstream profiles. Again, the windstorm is suppressed. In Fig. 8c, the stratosphere itself has been removed and replaced by a near-neutral layer. The windstorm is rather insensitive to this modification. Note that cases 8b, 8c have been first simulated by Durran (1986) with the same results. Finally, in Fig. 8d, the

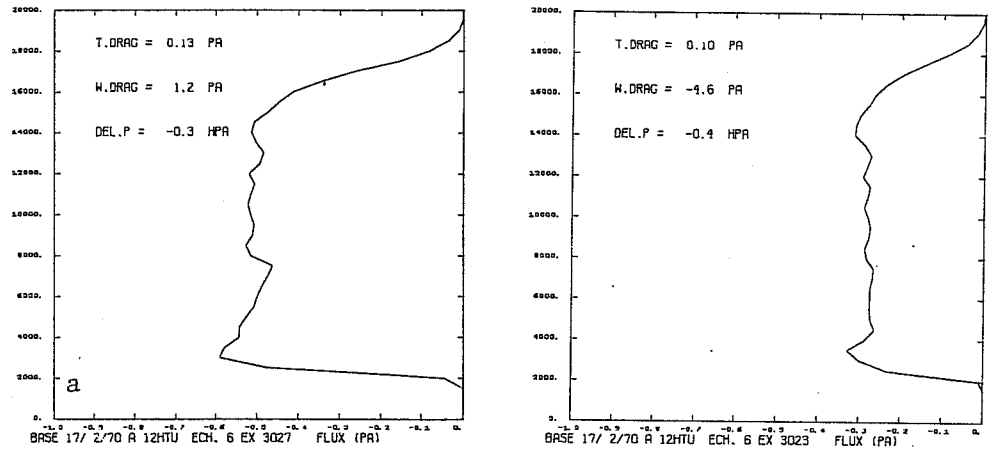

Fig. 7 Effect of 10% change in the maximum wind speed on the momentum flux (a) control run, (b) modified.

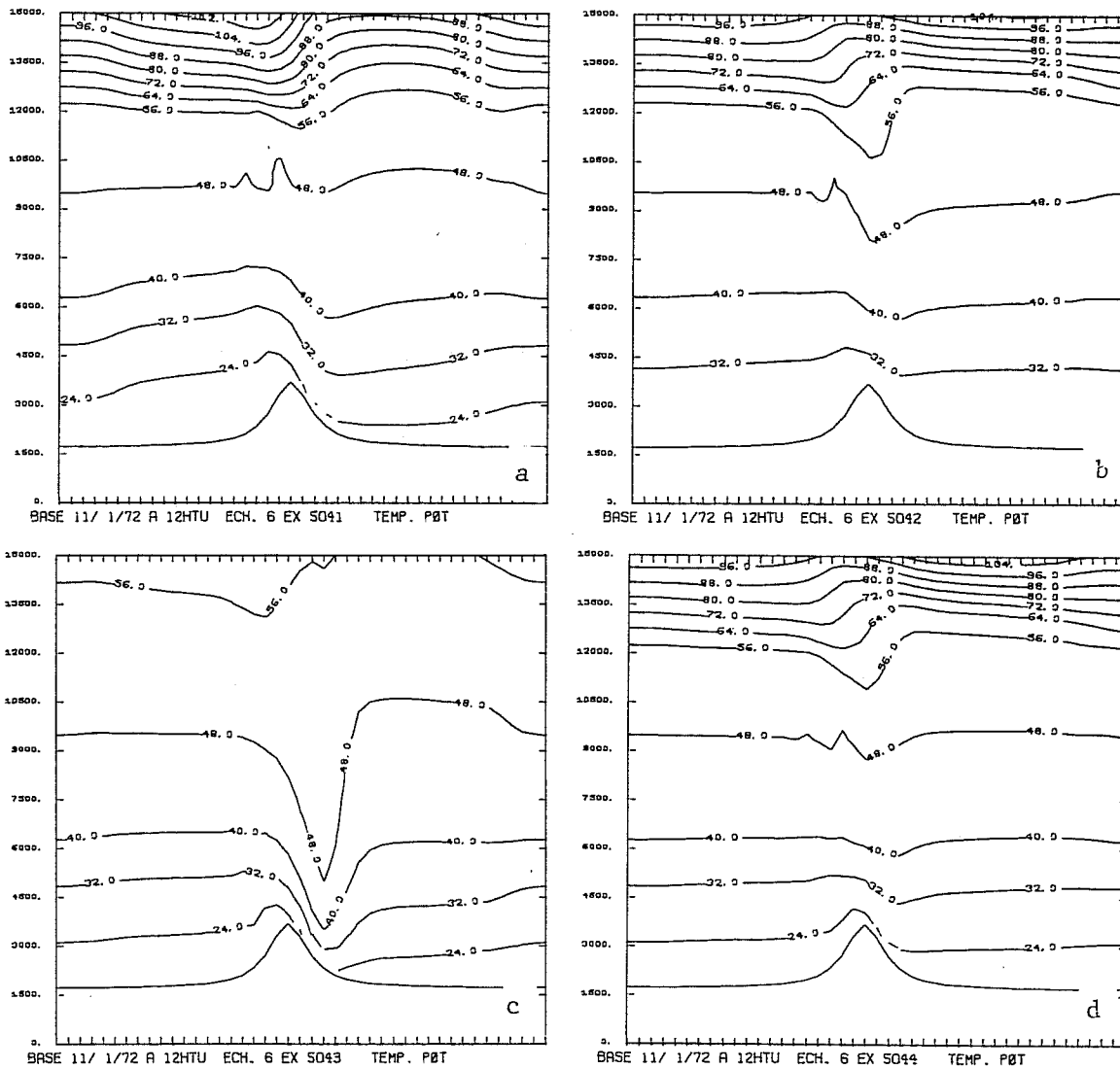

Fig. 8 Vertical cross-section of the potential temperature for various modifications of the upstream profiles, case of 11/01/72, see main text.

wind in the low-level inversion has been decreased from 15 m/s to 10 m/s. Again, the wind-storm is suppressed.

5.2 Sensitivity to the formulation of the horizontal diffusion

This is best highlighted by comparing results using the operational formulation (θ along σ-surfaces) with the one adopted here (T along p-surfaces), with the same value of K_2. Such a comparison is shown for the vertical flux of momentum in Fig. 9 of case 4.1 (Note that this is not the same upstream profile as for the control run). When the new formulation is used (9a) the flux is constant throughout the troposphere, whereas with the operational formulation (9b), it decreases markedly, contrary to the observation. Moreover, when no diffusion at all is used, the result is very close to Fig. 9a.

The flaw introduced by the use of the formulation along σ-surfaces reaches a still higher degree on case 4.3 (11.01.1972). Indeed, the sensitivity studies described in 5.1 were reproduced with the σ-surface diffusion: in all cases, the model produced a strong windstorm, at variance with the cited reference studies. Thus, just because of a wrong formulation of the horizontal diffusion, the model loses its ability to discriminate between cases where a windstorm should occur, and those where it should not. Of course, the sensitivity runs were also reproduced without any diffusion at all, and the results were the same as discussed under 5.1.

5.3 Sensitivity to the amount of dissipation

The sensitivity to the value of K_2 in the horizontal diffusion has also been investigated. The value used in the control run $K_2=6\Delta X$ x (6 m/s) corresponds to a quite high value, which turned out to be necessary to have a stationary solution in case 4.3. For smaller values of K_2, the hydraulic jump occurring downstream of the crest was able to move downstream until it was blocked by the lateral boundary condition, a clearly unphysical solution. This calls for further research to determine when and where the horizontal diffusion, and more generally, energy dissipation, should be large in this kind of flow. Indeed, when horizontal resolution increases, there is a clear need to link the value of K_2 to the physical processes occurring at subgrid-scale. This could be achieved by taking advantage of existing schemes to forecast the subgrid-scale turbulent kinetic energy (e.g. the Therry and Lacarrère (1983) scheme, already used in several mesoscale models).

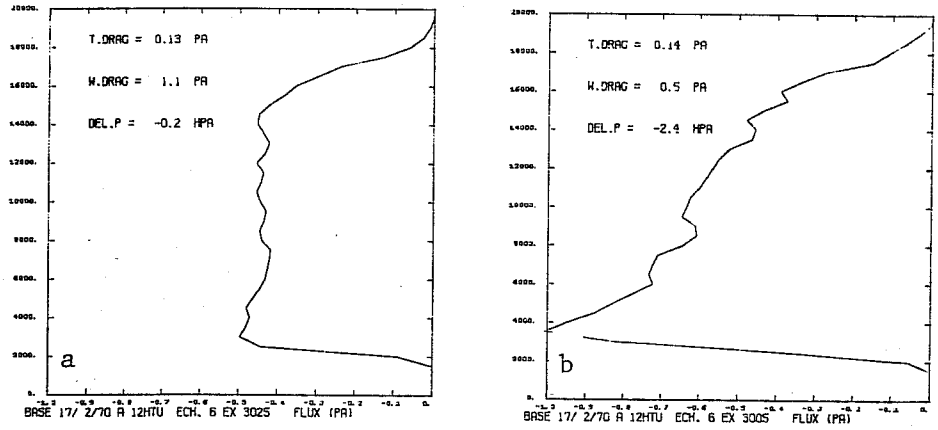

Fig. 9 Vertical flux of momentum for horizontal diffusion along p-surface (a), and along σ-surface (b).

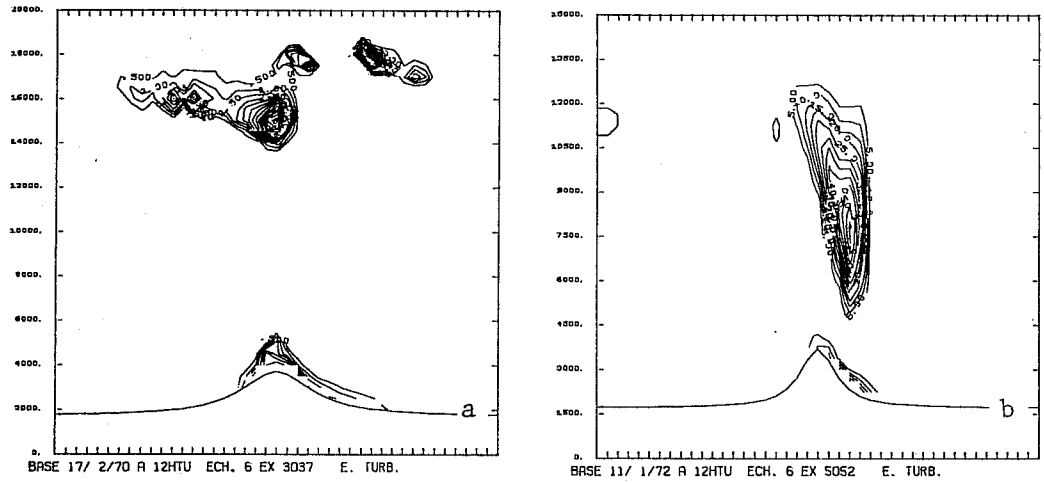

Fig. 10 Vertical cross-section of turbulence kinetic energy for 17/2/70 (a) and 11/01/72 (b)

To illustrate the potential benefits of this approach, preliminary results recently obtained with this scheme are shown in Fig. 10. They are TKE vertical cross-sections for cases 4.1 and 4.3. On case 4.1 (Fig. 10a), the TKE has large values in the blocking region below the tropopause, where near-neutral stability is encountered. On case 4.3 (Fig. 10b), the TKE reaches very large values in the highly sheared and near-neutral flow associated to the tropopause folding and to the hydraulic jump. The maximum predicted value is larger than 50 $(m/s)^2$, (Lilly claims a value of 150 $(m/s)^2$ for this case).

Finally, the value of the roughness length Z_0 has been found to be a controlling parameter for the occurrence of the windstorm. Let us remember that the control run uses Z_0 = 0.04 m. For values of Z_0 between 0.04 m and 0.2 m, the windstorm was delayed but still occurred. For Z_0 0.2 m it was suppressed. This is in contradiction with currently admitted values of the roughness in mountainous areas, and calls for further research on the specification of this important parameter.

6. CONCLUSIONS

As horizontal resolution increases, hydrostatic, primitive-equation models similar to the one used in ECMWF can reach an increased ability to deal with orographic flows. The results presented here show that these models can indeed perform very well, if a few constraints are respected. They are:

(i) A good vertical resolution. Although a resolution as good as the one used here (ΔZ=500 m) is not required, the model results start to degrade significantly when ΔZ=1 km is not achieved throughout the model's useful atmospheric depth.

(ii) A damping layer at the top of the model, or a radiating UBC.

(iii) A formulation of the horizontal diffusion along true horizontal surfaces.

(iv) The best possible specification of the upstream profiles; this calls for refinement in the vertical resolution of the analysis.

Furthermore, the sensitivity experiments call for further research and experimentation in the following domains:

(i) Definition of diffusion coefficients variable in space and time, to account for the physical variability of the dissipative processes. This could be achieved by

(ii) development of a subgrid-scale turbulence kinetic energy prognostic equation.

(iii) research on the definition and the possible mapping of the roughness length in mountainous areas.

References

Alaka, M.A., Ed., 1960: The airflow over mountains. WMO Tech. Note 34, 135 pp.

Bougeault, P., 1983: A non-reflective upper boundary condition for limited height hydrostatic models. Mon.Wea.Rev., 111, 420-429.

Bougeault, P., 1986: Le modèle Péridot Une étude de qualification à méso-échelle. Note de travail de l'EERM, n°168.

Bougeault, P., 1987: Etude de quelques écoulements orographiques à l'aide du modèle Péridot. lère partie: qualification du modèle. Note de travail de l'EERM, n°191.

Bougeault, P., 1987b: Simulation numérique d'ondes de relief hydrostatiques bidimensionnelles. Proceedings AMA87, CNRM, Toulouse, 19-20 octobre 1987, pp 23-34 (available from CNRM, Toulouse).

Brière, 1987: Energetics of day time sea breeze circulation as determined from a two-dimensional third-order turbulence closure model. J.Atmos.Sci., 44, 1455-1474.

Cariolle, D., 1987: L'influence des ondes de gravité d'origine orographique sur la circulation générale: Résultats du modèle Emeraude 30 niveaux. Proceedings AMA87, CNRM, Toulouse, 19-20 octobre 1987, pp 121-128 (available from CNRM, Toulouse).

Durran, D.R. and J.B. Klemp, 1983: A compressible model for the simulation of moist mountain waves. Mon.Wea.Rev., 111, 2341-2361.

Durran, D.R., 1986: Another look at downslope windstorms. Part I: The development of analogs to supercritical flow in an infinitely deep, continuously stratified fluid. J.Atmos.Sci., 43, 2527-2543.

Durran, D.R., 1987: Another look at downslope winds. Part II: Non linear amplification beneath wave-overturning layers. To appear in J.Atmos.Sci.

Enquist, B. and A. Majda, 1977: Absorbing boundary conditions for the numerical simulation of waves. Math.Comp., 31, 629-651.

Enquist, B. and A. Majda, 1979; Radiation boundary conditions for acoustic and elastic wave calculations. Comm.PureAppl.Math., 32, 315-337.

Garner, S.T., 1986: A radiative upper boundary condition adapted for f-plane models. Mon.Wea.Rev., 14, 1570-1577.

Hoinka, K.P., 1985: A comparison of numerical simulation of hydrostatic flow over mountains with observations. Mon.Wea.Rev., 113, 719-735.

Imbard, M., A. Joly and R. Juvanon du Vachat, 1986: Le modèle de prévision numérique Péridot: Formulation dynamique et modes de fonctionnement. Note de travail de l'EERM n°161, 70 pp.

Klemp, J.B. and D.K. Lilly, 1975: The dynamics of wave-induced downslope winds. J.Atmos.Sci., 32, 320-339.

Klemp, J.B. and D.K. Lilly, 1978: Numerical simulation of hydrostatic mountain waves. J.Atmos.Sci., 35, 78-107.

Klemp, J.B. and D.R. Durran, 1983: An upper boundary condition permitting internal gravity wave radiation in numerical mesoscale models. Mon.Wea.Rev., 111, 430-444.

Klemp, J.R. and D.R. Durran, 1987: Numerical modelling of Bora winds. Meteor.Atmos.Phys., 36, 215-227.

Lilly, D.K. and P.J. Kennedy, 1973: Observations of a stationary mountain wave and its associated momentum flux and energy dissipation. J.Atmos.Sci., 30, 1135-1152.

Lilly, D.K., 1978: A severe downslope windstorm and aircraft turbulence event induced by mountain wave. J.Atmos.Sci., 35, 59-77.

Louis, J.F., M. Tiedtke and J.F. Geleyn, 1981: A short history of the operational PBL-parameterization of ECMWF. Workshop on Planetary Boundary Layer Parameterization, ECMWF, 25-27 November, 1981, pp. 59-79.

Peltier, W.R. and T.L. Clark, 1979: The evolution and stability of finite amplitude mountain waves. Part II: Surface wave drag and severe downslope windstorms. J.Atmos.Sci., 36, 1498-1529.

Petré, P., 1987: Contribution à l'étude du Bora utilisant les données avions de l'expérience ALPEX. Note de travail de l'EERM, n°172.

Rasch, P.J., 1986: Toward atmospheres without tops: Absorbing upper boundary conditions for numerical models. J.Roy.Met.Soc., 112, 1195-1218.

Schumann, U., T. Hauf, H. Holler, H. Schmidt and H. Volkert, 1987: A mesoscale model for the simulation of turbulence, clouds and flow over mountains. Formulation and validation examples. Contr.Atmos.Phys., 60, 413-446.

Smith, R.B., 1985: On severe downslope winds. J.Atmos.Sci., 42, 2597-2603.

Therry, G. and P. Lacarrère, 1983: Improving the eddy kinetic energy model for planetary boundary layer description. Bound.LayerMeteoro., 25, 63-88.